

Biogas-powered small power generation system designed for the agricultural sector to support the BCG model in Thailand

Panupon Trairat^{*1)}, Sakda Somkun¹⁾, Tanakorn Kaewchum¹⁾, Tawat Suriwong¹⁾, Pisit Maneechot¹⁾ and Tanongkiat Kiatsiriroat²⁾

¹⁾School of Renewable Energy and Smart Grid Technology (SGtech), Naresuan University, Phitsanulok, Thailand

²⁾Department of Mechanical Engineering, Faculty of Engineering, Chiang Mai University, Chiang Mai, Thailand

Received 15 April 2023

Revised 1 September 2023

Accepted 26 September 2023

Abstract

This study presents the design of a small grid-connected power generation unit for farming systems to support the Bio-Circular-Green Economic Model (BCG) in Thailand. We focus on using the remaining agriculture waste resources to be reused according to the circular economy in the BCG model. Biogas was used as the primary fuel for an internal combustion engine, with gasoline and LPG as the immediate emergency reserves. We have integrated an engine to transmit power to a self-excited induction generator and designed a grid-connected inverter control strategy based on PQ control for the power conversion of the system by using digital signal processing. Using interface-based Internet of Things, devices can be wirelessly connected for control and logging data via a dashboard application.

Keywords: Biogas, Self-Excited Induction Generator, Internal combustion engine, BCG model, Circular economy

1. Introduction

Thailand has the majority of its people engaged in agriculture: annual crops such as rice, sugar cane, corn, cassava, etc., and small livestock farming such as pigs, chickens, fish, cows, etc., and so is considered an agricultural society. But the farm production process is still at a low level. Due to the small number of innovations related to agriculture, the Thai government supports innovation to improve the quality and quantity of agricultural production and has presented a Bio-Circular-Green Economic Model (BCG) model as a strategy to create sustainability and equality for the economy, society, and environment [1-3]. This model focuses on applying science, technology, and innovation to transform a comparative advantage in biodiversity and culture into a competitive one. Its benefits are concentrated in four strategic sectors: 1) Agriculture and Food, 2) Health and Medicine, 3) Energy, Materials, and Biochemistry, and 4) Tourism and Creative Economy. The BCG model consists of three leading economies: the Bio-Economy (B) system focuses on the cost-effective use of biological resources, linking with the Circular Economy (C) that implements the reuse of various materials as much as possible, and both these economies are within the Green Economy (G) system which aims to solve pollution problems to sustainably reduce the impact on the planet [4-6], as shown in Figure 1. Furthermore, the BCG model will drive smart practices for Agriculture 4.0 to make agriculture in Thailand more sustainable [3-6].

According to the chapters in the 2021-2027 BCG Action Plan [1], two main issues for development in the agriculture and energy sectors are pushing for renewable energy. Biogas is an engaging alternative energy for recycling waste from agricultural and industry in accordance with the circular economy based on the BCG model [1, 7]. When we surveyed Thailand's agricultural and livestock sectors, there was a potential for biogas fuel production from agricultural waste or animal manure [8-10], which have been used in terms of burning fuel for cooking. Biogas is an attractive fuel for power generation but is not widespread. Supposing it can generate electricity for agriculture, it will increase self-sufficiency by managing agricultural and household electricity use. Biogas-fueled power generation can respond to three key points of the BCG model. This can be classified, for the sake of clarity, as follows: 1) Bio-economy: take biotechnology and biodiversity as a driver. 2) Circular economy: using waste materials to generate alternative energy. 3) Green economy: environmentally friendly and sustainable development.

This research aims to design a small-size grid-connected power generation integrated with a Self-Excited Induction Generator (SIEG) and an internal combustion engine (IC engine) using biogas as fuel. The system was developed focusing on using locally produced equipment that is generally available, resulting in simple maintenance. We selected an IC engine to be the prime mover for the generator. Since farmers use it daily for farm use, such as water pumping and filling, it can be applied in another application without complicated modifications to be used with a biogas fuel. We designed a back-to-back converter with a capacitor bank to control power conversion from an internal combustion (IC) engine to an SEIG. We connected it to the grid with a DC-link size of 400 V, with the maximum output power from the converter being 1.5 kW. The system to measure, process, and communicate was added through an IoT system displayed on a mobile application dashboard to manage the electricity used. The experimental design was split into two tests: 1) Laboratory testing of the effectiveness of the SEIG, the inverter, and the control system. The test system was connected to the

*Corresponding author.

Email address: panupont61@nu.ac.th

doi: 10.14456/easr.2023.57

grid at a power rating of 1.5 kW, and the system was run on gasoline 95 fuel. 2) The engine's performance when using three different types of fuel (95-octane gasoline, LPG, and biogas) was tested, including greenhouse gas emissions.

2. Closed-loop circular economy systems for the agricultural sector

The circular economy for agriculture refers to an approach that aims to create a closed-loop system within the agricultural sector, minimizing waste, maximizing resource efficiency, and promoting sustainable practices. [4-7]

This concept draws its inspiration from natural ecosystems, where waste from one process becomes a valuable input for another, creating a closed-loop system that maximizes resource utilization and reduces environmental impact. Here is how it can be applied to agriculture:

1) Waste Reduction and Valorization:

- Implement composting and anaerobic digestion to convert organic waste (crop residues, food scraps) into nutrient-rich compost and biogas.

- Recycle agricultural byproducts and residues as feedstock for bioenergy production or other value-added products.

2) Closed-loop Systems:

- Integrate livestock farming and crop production, where animal waste becomes a nutrient source for crops and crop residues become feed for animals.

- Creating integrated farming systems where livestock waste is used as a resource rather than a pollutant. For example, using manure as fertilizer or converting it into biogas for the sake of producing energy.

Figure 1 shows the closed-loop circular economy systems for the agricultural sector. The red arrow closed-loop demonstrates the purpose of this study. It can be briefly explained as follows: Agricultural and livestock waste is fermented in tanks by an anaerobic digestion process. The resulting product is the required methane (CH₄) gas and other gas components. The remainder from the completion of this process will be organic fertilizer, which will be used as plant food. The resulting methane gas is converted into heat and electrical energy.

Thailand has always used a closed-loop system to reduce waste by producing biogas from agricultural and livestock waste and occasionally using it as fuel for burning. However, electricity power generation from biogas was still not widely used. Producing electricity from biogas will contribute to this system's completion and can lead to a more resilient, efficient, and sustainable energy system that balances economic prosperity with environmental and social well-being in Thailand.

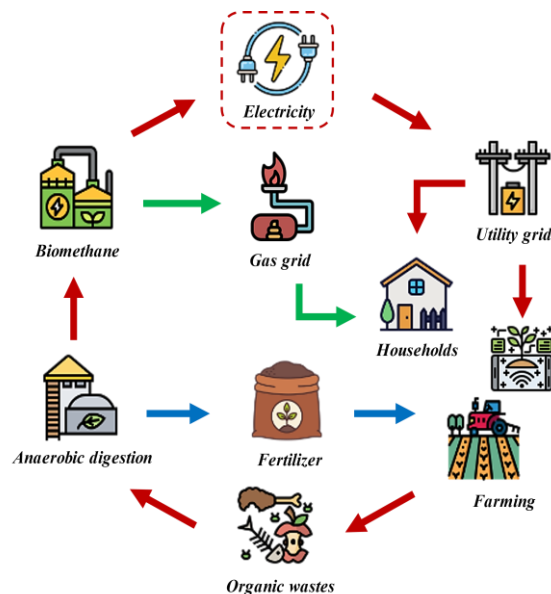


Figure 1 Closed-loop circular economy system for the agricultural sector [4-7]

3. Biogas production and potential in Thailand

Biogas production is a sustainable and renewable energy generation process that involves the conversion of organic materials into biogas through the process of anaerobic digestion. Biogas primarily consists of methane (CH₄) and carbon dioxide (CO₂), along with trace amounts of other gases like hydrogen sulfide (H₂S) and water vapor. It can be used as a source of energy for various applications, including generating electricity, heating, and even as a vehicle fuel [8-10].

Here are the key steps involved in biogas production:

- 1) **Feedstock Selection:** Organic materials, known as feedstock, are used as the raw materials for biogas production. Common feedstock sources include animal manure, agricultural residues, food waste, sewage sludge, and energy crops (such as maize or grass).
- 2) **Preparation:** The feedstock is collected and prepared for the anaerobic digestion process. This may involve shredding, chopping, or other mechanical processes to reduce particle size and increase the surface area for microbial activity.
- 3) **Anaerobic Digestion:** Anaerobic digestion is the core process, in which microorganisms break down the organic matter in the absence of oxygen. This occurs in a sealed, oxygen-free digester tank. It has four main stages:
 - **Hydrolysis:** Complex organic materials are broken down into simpler compounds.
 - **Acidogenesis:** Acid-forming bacteria convert the simpler compounds into volatile fatty acids.

- **Acetogenesis:** Acetic acid is formed from the volatile fatty acids.
 - **Methanogenesis:** Methanogenic bacteria convert the acetic acid and other intermediates into methane and carbon dioxide.
- 4) **Gas Collection:** The biogas produced during the anaerobic digestion process is collected at the top of the digester tank.
 - 5) **Gas Storage and Upgrading:** Biogas may require further treatment to remove impurities such as hydrogen sulfide (H₂S) and moisture. Additionally, it can be stored in tanks or used directly for various applications. In some cases, it can also be upgraded to biomethane, which is a purified form of biogas with a higher methane content suitable for injection into natural gas pipelines or use as a transportation fuel.
 - 6) **Biogas Utilization:** Biogas can be used for a wide range of applications, including:
 - **Electricity Generation:** Biogas can be used in gas engines or turbines to generate electricity.
 - **Heat Production:** It can be used for heating purposes in homes, industries, or for district heating.
 - **Vehicle Fuel:** When upgraded to biomethane, it can be used as a clean-burning fuel for vehicles.
 - **Cooking and Lighting:** In some regions, biogas is used for cooking and lighting in households.

Biogas production offers several environmental and economic benefits. It helps to manage organic waste, reduce greenhouse gas emissions, and provides a renewable source of energy. Additionally, it can be integrated into sustainable agricultural and waste management practices, contributing to a circular economy. However, the success of biogas production depends on factors like feedstock quality, digester design, and operational management.

Khotmanee and Pinsopon [8] studied the potential for biogas production in Thailand. By surveying data for three sectors, industrial plants, agricultural plants, and livestock in 2019, it was found that Thailand has the potential to produce a total of 22826.79 million cubic meters per year, divided into industrial plants at 7521.48 million m³ per year, agricultural plants at 14479.01 million m³ per year, and livestock at 826.30 million m³ per year. More details are shown in Table 1.

Table 1 Potential biogas production in Thailand 2019 [8]

Biogas Source	Production potential (million m ³ /years)	Productivity (million m ³ /years)	Remaining (million m ³ /years)
Industrial plants	7,521.48	747.45	6774.03
Livestock	826.30	68.61	757.66
Agricultural	1,4479.01	-	14,479.01
Total	22,826.79	816.06	22,010.70

For this research, only the agriculture and livestock sectors were studied. We therefore show the rates of waste-to-biogas production in these two sectors according to the type of agricultural plants and livestock farms found in Thailand, as shown in Tables 2 and 3 [8], [10].

Table 2 Livestock biogas production rate [8]

Types	Manure rate per day (kg/animal)	Manure collected (%)	Evaporation Rate of Solids (%)	Biogas Production Rate (m ³ /kg(solids))
1. Beef cattle	5.00	50	13.37	0.307
2. Dairy Cattle	15.00	80	13.37	0.307
3. Breeder Pigs	2.00	80	24.84	0.217
4. Piglets	0.50	80	24.84	0.217
5. Fattening Pigs	1.20	80	24.84	0.217
6. Chickens	0.03	80	23.34	0.242

Table 3 Agricultural waste biogas production rate [8]

Type	Waste	Ratio of Waste to product mass (%)	Waste Unused Percentage (%)	Biogas production rate (L/kg(dry))	Dry Material to Raw Material (%)
1. Rice	Straw	29.37	39.40	162 (Fresh)	-
2. Corn	Trunk	43.52	73.71	250	70
	Leaves	30.97	100	225	90
	Stubble	21.26	73.64	344	90
3. Sugarcane	Leaves and Shoots	39.51	93.24	262	70
4. Cassava	Stems and Leaves	28.93	14.87	274	65
	Rhizome	17.12	90.25	141	65

4. Materials and methods

In this study, an SIEG) and an IC engine using biogas as fuel are integrated to create a small grid-connected power generation system. The system's development was centered on utilizing widely accessible, locally produced equipment, which makes maintenance easy. We chose the generator's IC engine as the prime mover. Since it is often used by farmers for farming purposes, such as water pumping and filling, it can be utilized in another application with simple adjustments to be used with biogas fuel. To manage power conversion from an IC engine to a SEIG, we devised a back-to-back converter with a capacitor bank. A grid-connected inverter with a controller embedded inside was developed to power conversion and synchronize power to the grid, and it can be monitored and controlled via a smartphone application, as shown in Figure 2.

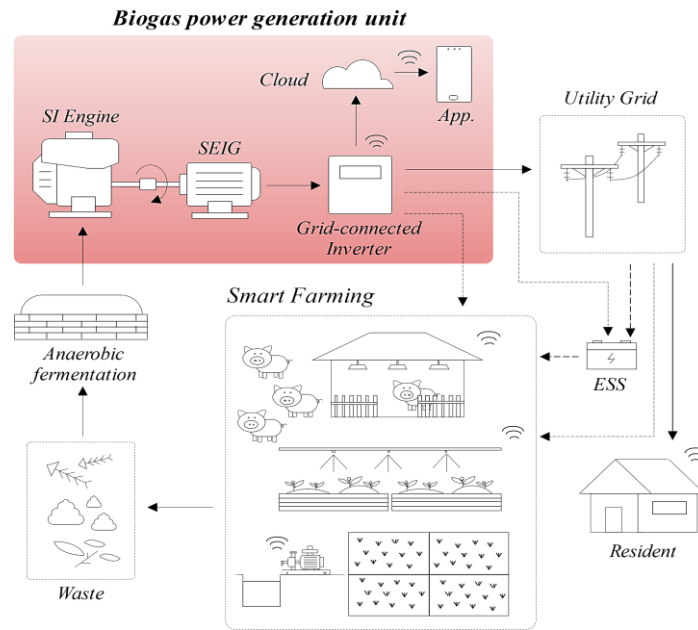


Figure 2 Proposed biogas power generation unit system

4.1 Internal combustion engine selection and modification

Gasoline-powered IC engines are suitable for the direct use of biogas [11-13]. The gas hose is installed in the carburetor area in a position above the accelerator by connecting the biogas pipe. A valve is installed outside to control the amount of biogas sent to the combustion chamber, as shown in Figure 3. This modification of the engine from the original carburetor (which mixes gasoline with air) incorporates air with biogas instead. The machine can run on 100% biogas throughout its operation [14].

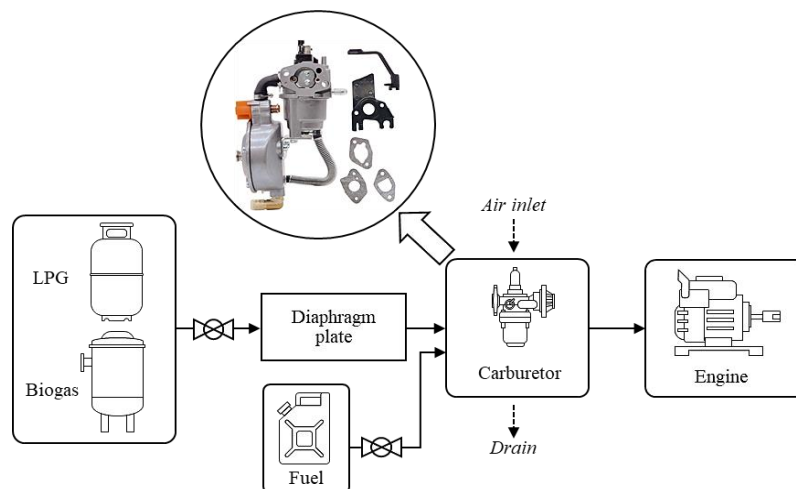


Figure 3 Biogas and LPG supply system for IC engine.

This work chooses a Honda GX200T2 QHT [15], a small four-stroke IC gasoline engine with a horizontal shaft. Air-cooled, it delivers a maximum power of 4.1 kW at 3,600 rpm and a maximum torque of 12.4 Nm at 2,500 rpm according to SAE J1349 standards. The dual fuel carburetor also allows the engine to accept biogas [15] LPG/ biogas when the engine is started. Negative pressure is supplied to the pressure regulating valve through the mixer. The seal arm swings to open the valve, and combustible gas enters the engine after decompression. The pressure regulating valve closes at the same time, and the combustible gas will stop when the engine shuts down.

4.2 Self-excited induction generator selection with DC-to-DC power conversion

A squirrel cage induction motor is suitable for direct coupling with the IC engine [16-18], where the operation speed is around 3000 RPM. This study selected a HITACHI TFO-K series [19], 220 V/ 380 V 2.2 kW two-pole three-phase induction motor as an SEIG. The designed system connects to an output voltage of 220 V and a frequency of 50 Hz, a low-voltage grid system. The inverter requires a minimum DC voltage of 311 V, so the output voltage and frequency of the generator must be properly regulated.

The generator requires reactive power to excite the strength of the magnetic field at the rotor core to generate a voltage at the terminals. The capacitor bank generates reactive power during the build-up, and when the load is connected, it continually uses the VSC-based PWM rectifier controlled by the PWM stage to impersonate this function [16, 18].

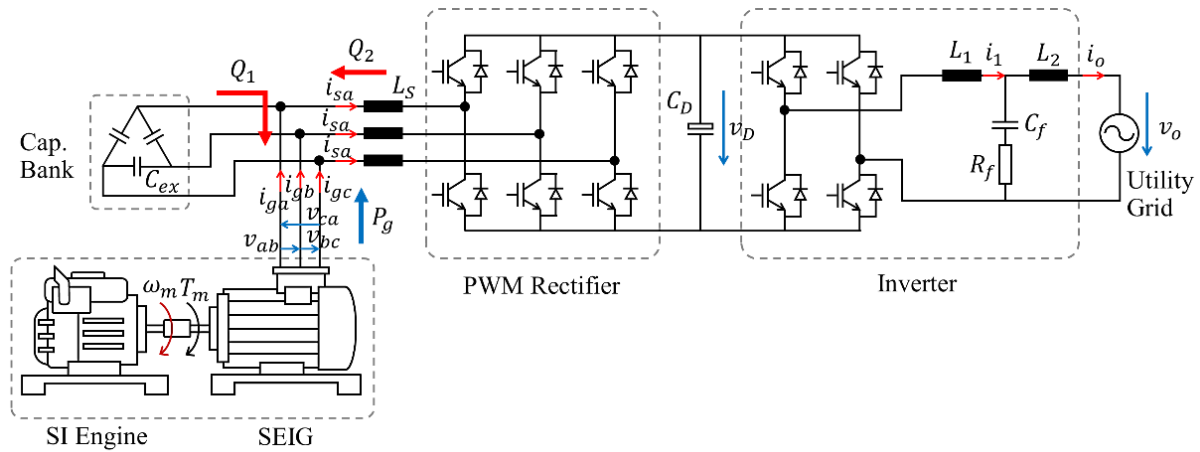


Figure 4 Proposed back-to-back converter with a capacitor bank

Figure 4 shows the topology of the proposed back-to-back converter. The SEIG with delta-connected windings generates a line-to-line AC voltage of 220 V, taking Q_1 from the capacitor bank. The VSC-based PWM rectifier boost-type converts the line-to-line voltage to v_D 400 VDC bus voltage. Then the v_D is converted to the required output voltage with an LCL active filter circuit to make it a pure sine before being fed to the grid [20, 21].

4.3 Power converter control structure

Figure 5 depicts the power converter control system. The SEIG-side and grid-side control schemes are implemented on a TMS320F28069 32-bit microcontroller from Texas Instruments [22]. The voltage and current signals of the SEIG and grid are sampled via the embedded analog-to-digital converters (ADCs), from which the control schemes generate the switching signals from the PWM units for the IGBTs via the gate driver circuits. The SEIG and capacitor bank are three-phase AC voltage sources with a star connection. The shaft rotational speed is not required. The shaft speed can be estimated from the generator frequency ω_g for a supervisory control system, along with other mechanical parameters such as temperatures, biogas pressure, and flow rate [20, 21].

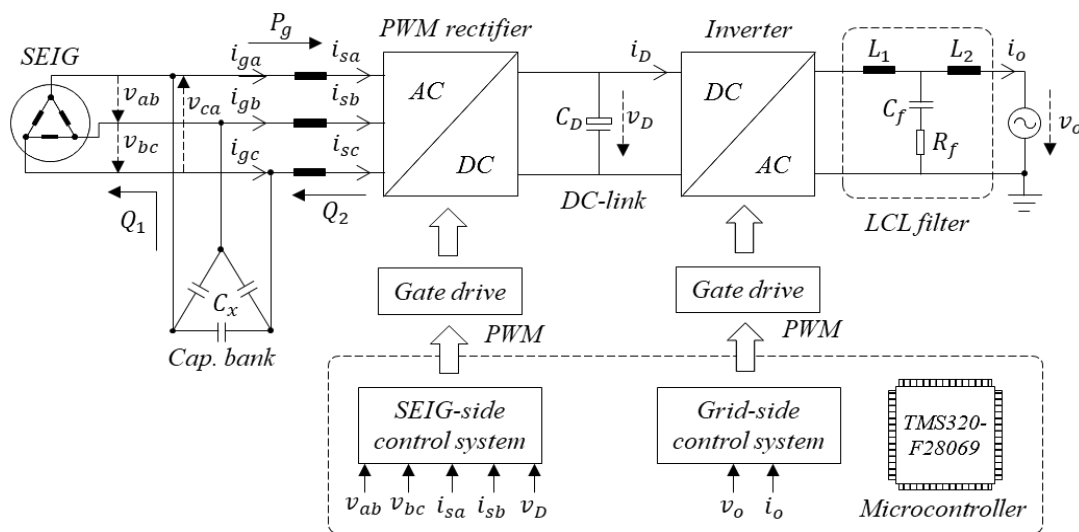


Figure 5 Power conversion topologies for the biogas power generation system design

The SEIG control scheme is implemented in the synchronous reference frame [20-23], so the active and reactive powers can be controlled separately. The control system of the PWM rectifier in the synchronous reference frame. A phase-locked loop (PLL) is used in this study [20, 21], which is implemented in the synchronous reference frame to estimate the angle and the frequency from the measured line-to-line voltages.

The output stage of the proposed topology in Figure 5 is the single-phase LCL-filtered grid-connected inverter. The damping resistor R_f of the LCL filter ensures control stability with the presence of a large grid impedance grid current (i) feedback control used in this study. The grid-side control system of the single-phase inverter is implemented in the multiple unbalanced synchronous reference frame on the same microcontroller with the SEIG-side control. The proposed control scheme consists of the fundamental component controller at the grid frequency and multiple harmonic controllers at frequencies. The harmonic controllers are used for the rejection of low-frequency voltage harmonics in the grid voltage and inverter output voltage due to switching dead times.

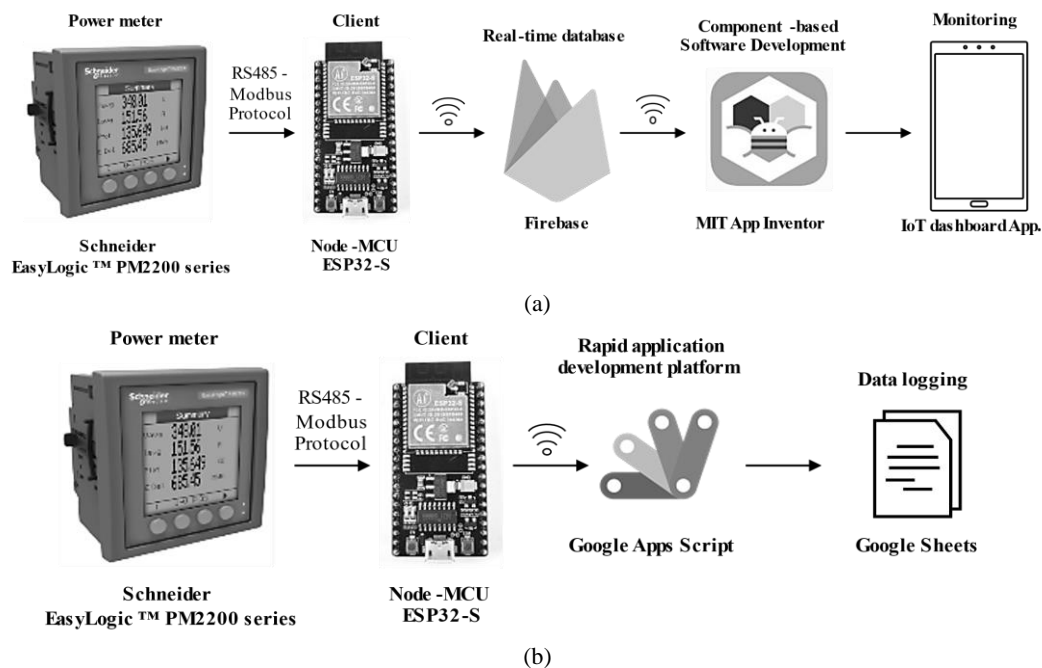
The proposed power converter in Figure 5 was constructed with the parameters listed in Table 4. The excitation capacitors C_x build up the SEIG voltage to the nominal value of $V_{LL} = 220$ V (line to line) at the no-load rotational speed approximately of 3,000 rpm. Assuming that the efficiency of the converter and SEIG is 70%, the nominal output power was set at 1.5 kW at which the mechanical input power $P_m = 2.14$ kW is close to the rated power.

Table 4 Parameters of the inverter

Symbol	Quantity	Value
P_o	Nominal output power	1.5 kW
V_{LLB}	Nominal SEIG line-to-line voltage	220 V
f_{gB}	Nominal SEIG frequency	50 Hz
C_{ex}	Excitation capacitors	40 μ F (Δ connection)
V_D	Nominal DC voltage	400 V
V_o	Nominal grid voltage	220 V
f_o	Grid frequency	50 Hz
f_c	Triangular carrier frequency	10 kHz
f_s	Sampling frequency	20 kHz
L_s	SEIG-side inductor	2 mH
C_D	DC bus capacitor	1000 μ F
L_1	LCL filter inductor	1 mH
L_2	Grid-side inductor	0.5 mH
C_f	LCL filter capacitor	3 μ F
R_f	LCL filter damping resistor	1 Ω

4.4 Designing the power monitoring system with IoT devices

The design of an electrical power display system based on a smartphone application is schematically shown in Figure 6(a). This research uses the *EasyLogic* PM2230 [24] power meter manufactured by Schneider Electric, which is used for industrial applications. Modbus protocol connection is supported by specifying the register location of the required parameters from the manufacturer's instruction manual. The data from the power meter is sent to the *NodeMCU* ESP32 via RS485 Modbus Protocol and converted to TTL (Transistor-Transistor Logic). It is forwarded via Wi-Fi to Google Firebase [25] as a real-time database for displaying windows on applications, by an application designed with MIT app inventor software developed on the MIT platform using Component Oriented Software (Component-based Software Development) principles without writing commands (Source code) [26, 27]. The real-time data collection system that is designed can be seen in Figure 6(b). We chose to collect the data on Google Sheets in real time every ten minutes. We created JavaScript code to retrieve the values sent from the *NodeMCU* ESP32 and store them in Google Sheets with the Google Apps Script function.

**Figure 6** Power Monitoring System based on the IoT: a) Power monitoring system on an application, and b) Realtime data logging.

5. Experimental setup

5.1 Experimental procedures

The experimental design was divided into two parts with different implications, namely, 1) laboratory testing, for testing the efficiencies of the SEIG, the inverter, and the control system. The system was operated on gasohol 95 fuel, with the test system connected to the grid at a power rating of 1.5 kW. 2) Field Test: to test and compare the engine performance using three types of fuel: gasohol 95, LPG, and Biogas, shown in Figure 7.

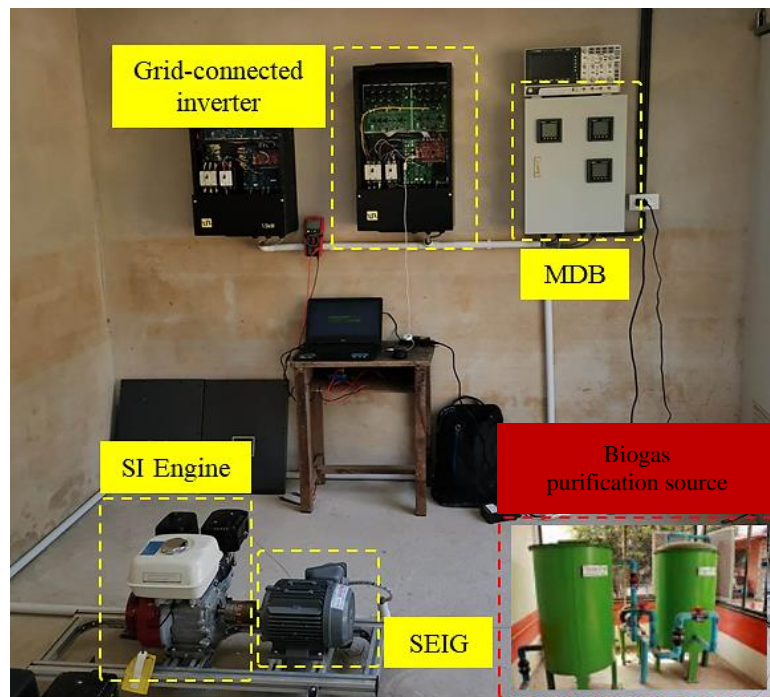


Figure 7 Experimental Setup of biogas generation unit

The performance of the prototype biogas power generation system was validated with biogas in the selected area, Ta Manoa Subdistrict, in December 2021. The composition of the biogas was monitored by an IRCD4 gas analyzer from Beijing Shi'An Technology Instrument during the experiment, as listed in Table 2. The engine's exhaust gas was also monitored using an SA500 gas analyzer from Beijing Shi'An Technology Instrument.

Figure 8 depicts the performance evaluation diagram of the prototype system. The tests used gasohol containing 90% of 95-octane gasoline and 10% ethanol by volume. The average thermal input power was determined from the consumption rate using a digital weighing scale monitored in ten-minute periods. LPG and biogas fueled the engine. Then the thermal input power was determined from the volumetric flow rate using a thermal mass flowmeter and the CH_4 content monitored by a gas analyzer. A torque-speed sensor was mounted on the shaft between the engine and the SEIG to measure the torque, speed, and mechanical power. A four-channel power analyzer measured the electrical parameters at the SEIG and converter outputs. A four-channel digital oscilloscope recorded the waveforms of the current and voltage.

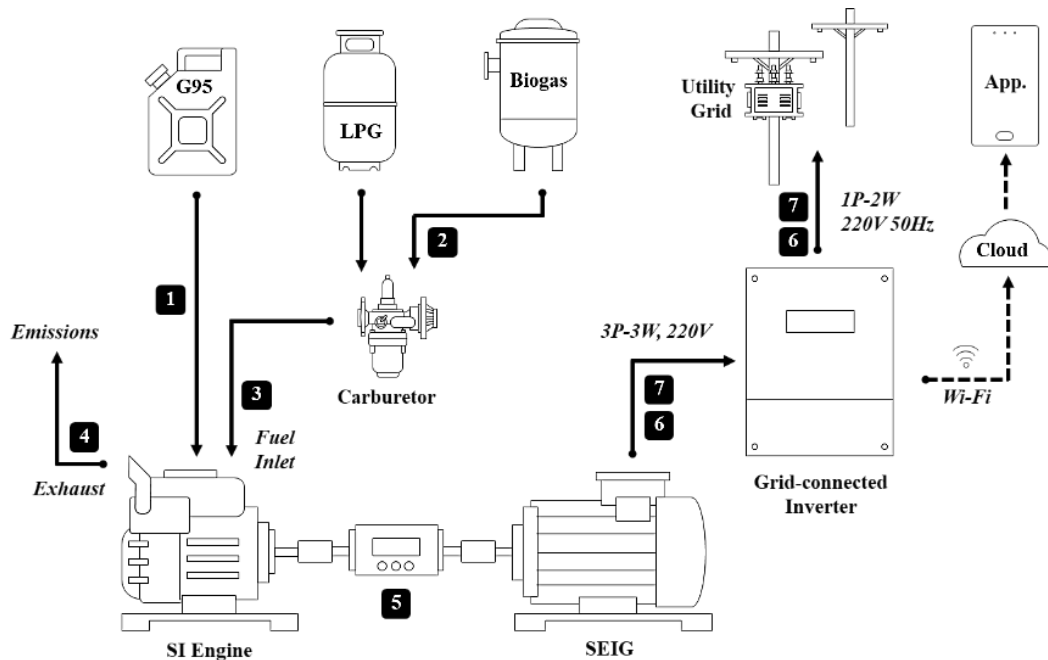


Figure 8 Schematic of experimental setup and measurement diagram of the proposed model: 1) Digital weighing scale, 2) Gas analyzer, 3) Flow meter, 4) Gas exhaust detection, 5) Torque/ speed sensor, 6) Digital power meter, 7) Four-channel digital oscilloscope

5.2 Calculation of overall system efficiency

The efficiency for the engines, generators, inverters, and systems can be calculated as follows [28, 29];

1) Engine performance (Efficiency of engine, η_{eng})

$$\eta_{eng} = \frac{\text{Mechanical power output}}{\text{Rate of fuel energy input}} \quad (1)$$

2) Generator performance (Efficiency of generator, η_{gen})

$$\eta_{gen} = \frac{\text{Electrical power output}}{\text{Mechanical power input}} \quad (2)$$

3) Inverter performance (Efficiency of inverter, η_{inv})

$$\eta_{inv} = \frac{\text{Electrical power output}}{\text{Electrical power input}} \quad (3)$$

4) System performance (Efficiency of system, η_{sys})

$$\eta_{sys} = \frac{\text{Net Electrical power output}}{\text{Rate of fuel energy input}} \quad (4)$$

6. Results and discussion

6.1 Engine performance

The test conditions with biogas were identical to the laboratory tests with gasohol. The no-load speed during the field experiments was set at approximately 3,250 rpm. The shaft speed with biogas drops at an output power greater than that with gasohol in the laboratory test. Thus, the excitation capacitors $C_{ex} = 40 \mu\text{F}$ were used in the field experiment in response to the higher no-load speed. For the field tests with biogas, the prototype system delivered a maximum output power of 1,200 W, 80% of the rated value due to low biogas production. The composition of the biogas in the field test is shown in Table 5.

Table 5 Biogas composition in the field experiments

Composition	Content
CH ₄	68.5%-70.0%
CO ₂	30%
H ₂ S	0.14%-0.24%

Figure 9 compares the efficiency of the engine with biogas, LPG, and gasohol 95 (G95). The engine efficiency with biogas is approximately 14.43% at an output power of 80%. The engine efficiency with biogas is expected to be about 15% at the rated power, estimated from the engine efficiency with gasohol and LPG curves.

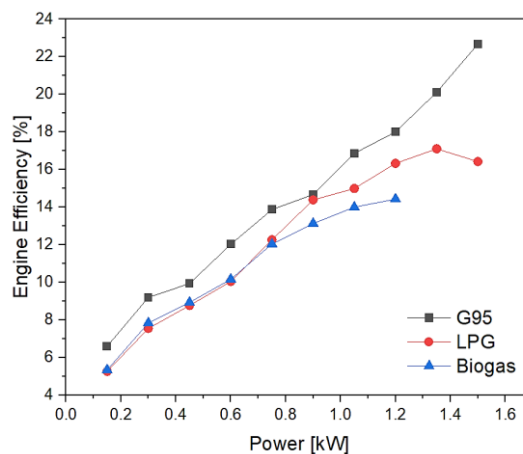


Figure 9 The engine efficiency with biogas gasohol and LPG curves

6.2 Generator performance

Figure 10 compares the generator of the engine with biogas, LPG, and gasohol 95 (G95). The generator efficiency with biogas is approximately 72.27% at an output power of 80%. The generator efficiency with biogas is expected to be about 73% at the rated power, estimated from the generator efficiency with gasohol and LPG curves.

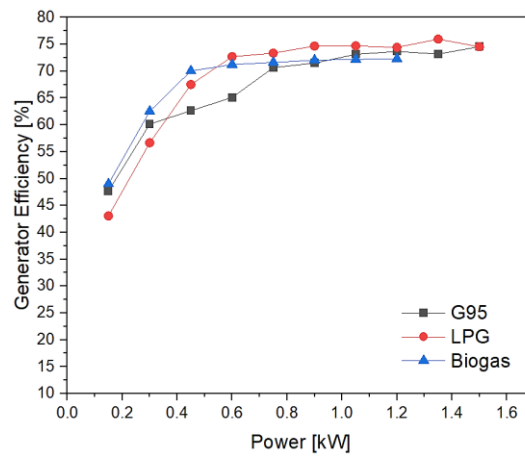


Figure 10 The generator efficiency with biogas gasohol and LPG curves

6.3 Inverter performance

Figure 11 compares the inverter of the engine with biogas, LPG, and gasohol 95 (G95). The inverter efficiency with biogas is approximately 95.33% at an output power of 80%. The inverter efficiency with biogas is expected to be about 96% at the rated power, estimated from the inverter efficiency with gasohol and LPG curves.

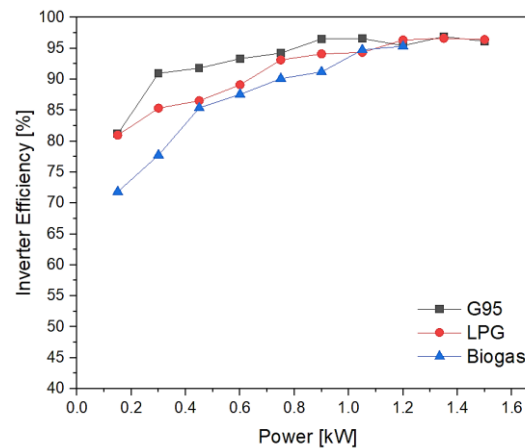


Figure 11 The inverter efficiency with biogas, gasohol, and LPG curves

6.4 System performance

Figure 12 compares the system of the engine with biogas, LPG, and gasohol 95 (G95). The system efficiency with biogas is approximately 10.65% at an output power of 80%. The system efficiency with biogas is expected to be about 13% at the rated power, estimated from the system efficiency with gasohol and LPG curves.

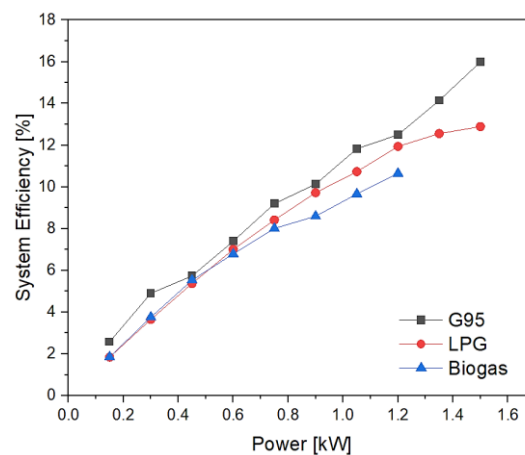


Figure 12 The system efficiency with biogas gasohol and LPG curves

6.5 CO and NO_x emissions

Figure 13 shows NO_x and CO emissions of the exhaust gas. The NO_x emission with biogas is far less than that with gasohol. The NO_x emission of the biogas-fed system is less than 50 ppm at 80% output power thanks to the purification process using the Fe(OH)₃ absorbent granules. Meanwhile, the CO emission of the biogas-fed engine decreases with the output power, where the CO emission is smaller than 400 ppm at 80% output power. This is believed to be due to there being a complete combustion process. On the other hand, the CO emission with gasohol is 2,000 ppm for every output power level. This indicates that the indicated values were limited by the measurable range of the exhaust gas analyzer, and the actual CO emission was above 2,000 ppm.

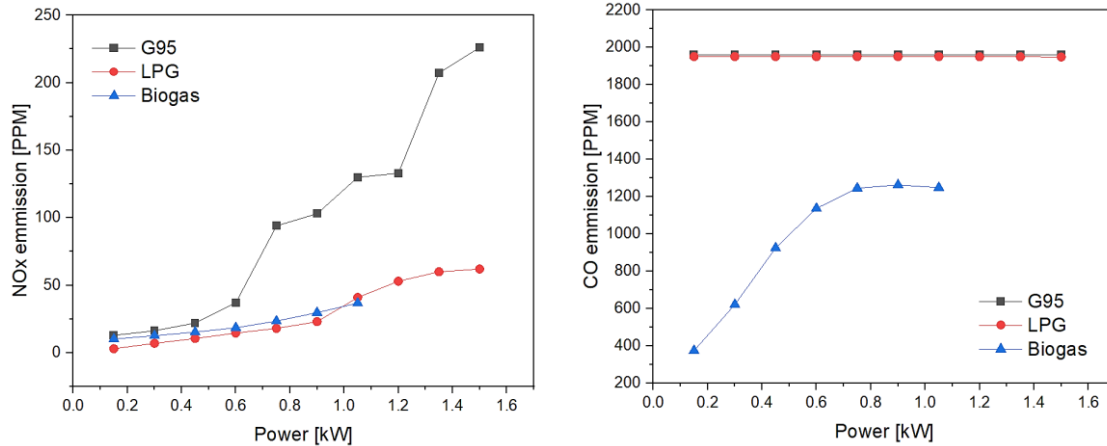


Figure 13 NO_x and CO emissions of the exhaust gas

6.6 Electrical power

The SEIG-side control system, Figure 14 displays the steady-state waveforms of the grid voltage $v_o(t)$ and current $i_o(t)$ and the SEIG voltage $v_{gab}(t)$ and $i_{ga}(t)$ at the rated output power of 1.5 kW. The grid current's waveform is nearly sinusoidal due to the added harmonic controller. The SEIG current's waveform is also nearly sinusoidal, which does not impose an additional loss due to current harmonics. The grid current harmonics comply with the IEEE 1547 Standard [20].

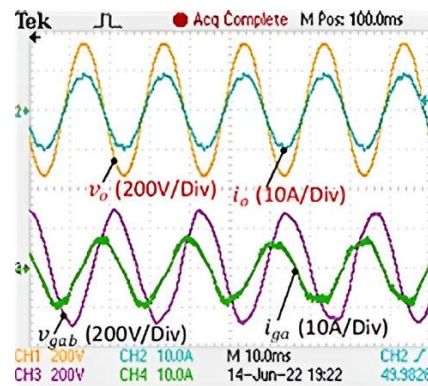


Figure 14 Steady state waveforms of the grid voltage and current and SEIG voltage and current.

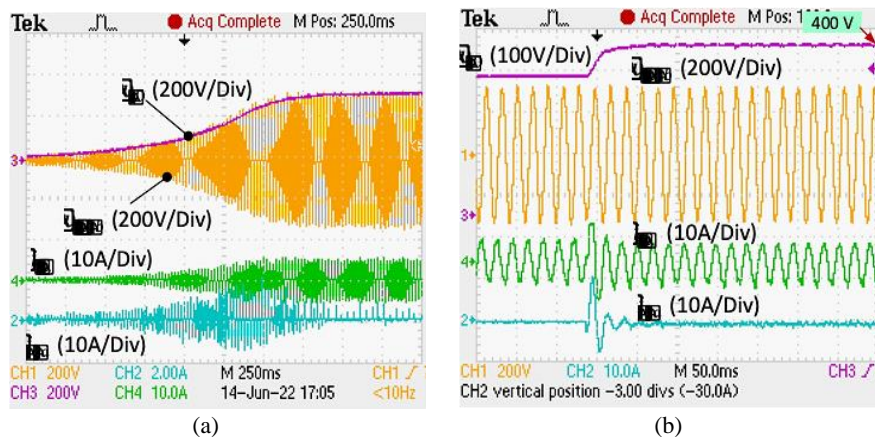


Figure 15 Transient voltage and current waveforms of the SEIG-side converter: (a) Voltage build-up period, (b) DC bus voltage startup period.

Figure 15(a) shows the SEIG voltage build-up period. In the beginning, there is a small SEIG voltage $v_{gab}(t)$ induced by the residual flux density in the rotor core, which is gradually increased due to the reactive power $q_1(t)$ from the capacitors C_{ex} . While building the terminal voltage, the SEIG also supplies active power to the DC bus capacitor C_D with the VSC operating as a passive rectifier. Figure 15(b) shows the startup of the PWM rectifier when $v_D(t)$ is increased to the reference $V_{Dref} = 400$ V. The voltage $v_{gab}(t)$ drops during the transient condition because the SEIG supplies the active power $p_g(t)$ to the bus capacitance. However, the SEIG is kept excited due to the reactive power $q_2(t)$ feeding back from the PWM rectifier to the SEIG.

6.7 Power monitoring system

This test used two power meters, a three-phase, three-wire delta ungrounded on the generator side and the second a one-phase, two-wire delta on the grid side as shown in Figure 16. The efficiency as determined from the data recorded in this experimental setup can be compared with that derived from the data recorded with the standard measuring equipment. Here, a power meter, model Chroma digital power meter 66204, is installed on the grid side to measure and record data every five minutes for comparison by setting the parameters V_s , I_s , and F_s . The comparison uses the square root of the mean squared error (RMSE) to evaluate of the error from the proposed data collection system. The comparison is shown in Figure 17.

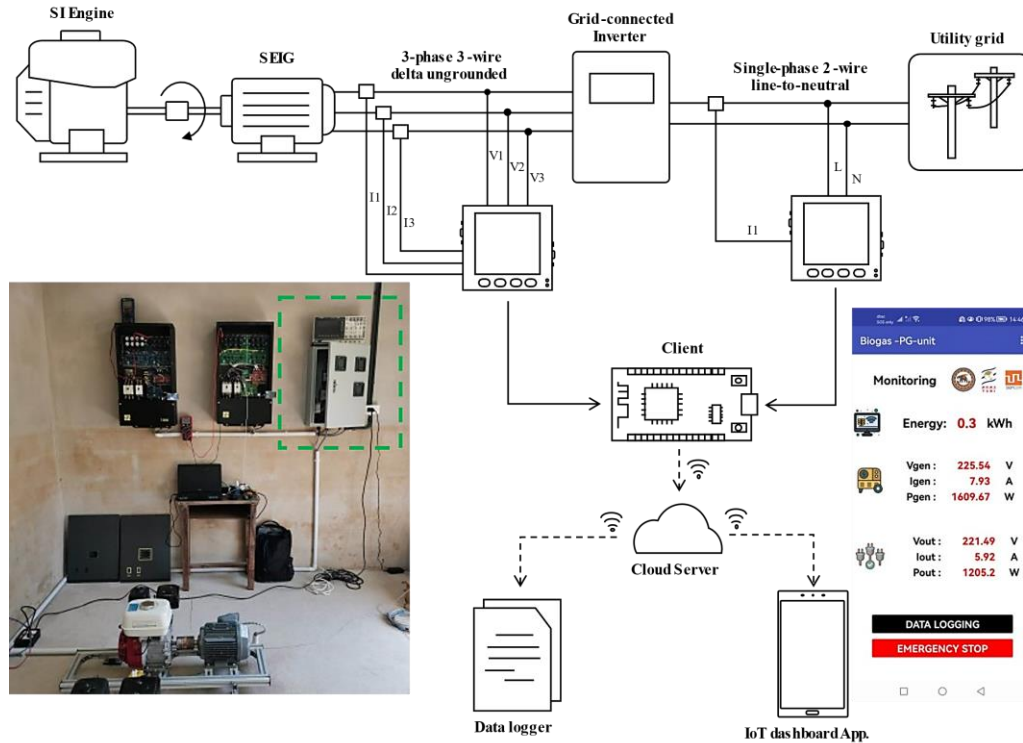


Figure 16 Power Monitoring System based on IoT

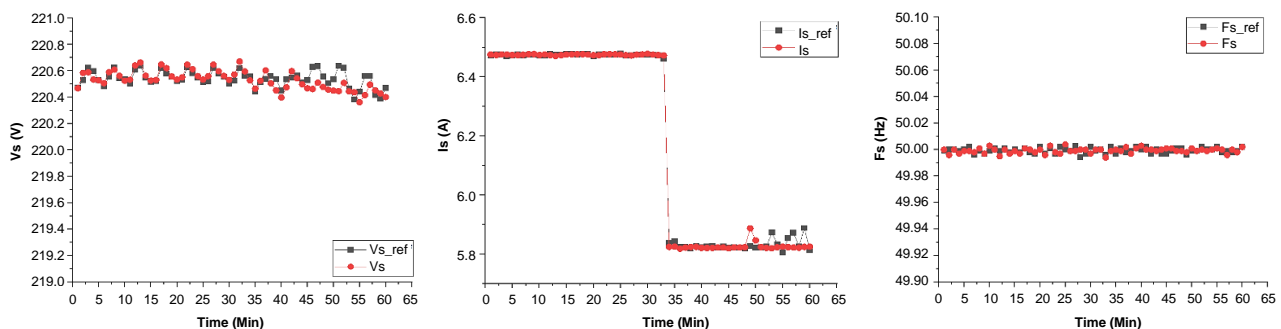


Figure 17 The errors from the proposed data acquisition system using RMSE

Figure 17, shows that the parameter data measured by the measuring instrument compared to the display system and the data collected in real-time were similar. When estimating the error values from the proposed data acquisition system using RMSE, it was found that the recorded grid voltage V_s , grid current I_s and grid frequency F_s tested had tolerances of 0.05888, 0.12547, and 0.00244 respectively, which are in the acceptable range and very close to those obtained by the standard measuring tools.

6.8 Analyzing biogas-fueled consumption in the proposed micro-power generation

In the previous test, we used one of the pig farm waste biogas sources mentioned in the section above. It was found to have a maximum power capacity of 1.2 kW. We analyzed the amount of pig manure required per hour for this farm. Based on the data from

Table 2, the results are as follows: The system requires 0.217 m³ of biogas per hour, equivalent to a minimum of 8.47 kg of raw materials per hour. Assume we want to produce electricity 8 hours per day at 1.2 kW. That means this pig farm needs to have at least 34 pigs.

In addition, we also analyzed and classified the required quantities of raw material for power generation at 1.2 kW per hour for other types of waste, from the agricultural and livestock sectors, as shown in Tables 6 and 7.

Table 6 Raw material for power generation at 1.2 kW per hour (Agricultural sector).

Type	Waste	Biogas Production rate (m ³ /kg(dry))	Required material (kg)	Dry material (kg)	Raw material (kg)	Product mass (kg)
1. Rice	Straw	0.162	6.83	6.83	6.83	58.99
2. Corn	Trunk	0.250	4.423	6.32	9.03	28.14
	Leaves	0.225	4.92	5.46	6.07	19.59
	Stubble	0.344	3.21	3.57	3.97	25.35
3. Sugarcane	Leaves and Shoots	0.262	4.22	6.03	8.617	23.38
	Stems and Leaves	0.274	4.04	6.21	9.557	222.06
4. Cassava	Rhizome	0.141	7.84	12.07	18.567	120.15

Table 7 Raw material for power generation at 1.2 kW per hour (Livestock sector).

Type	Biogas Production rate (m ³ /kg(solids))	Required material (kg)	Solid material (kg)	Raw material (kg)
1. Beef cattle	0.307	3.60	4.16	8.32
2. Dairy Cattle	0.307	3.60	4.16	5.20
3. Breeder Pigs	0.217	5.09	6.78	8.48
4. Piglets	0.217	5.09	6.78	8.48
5. Fattening Pigs	0.217	5.09	6.78	8.48
6. Chickens	0.242	4.57	5.96	7.45

6.9 Economic

The engine is programmed to run for eight hours each day, thus overall, there will be 14,600 hours of operation. A spark-ignition engine powered by biogas can run for up to 60,000 hours [30]. With a 7% interest rate, the five-year life-cycle cost (LCC) is USD 1046. Assume that poor biogas output and system maintenance result in a 10% system downtime. The following is then provided, with a 1.2 kW annual energy yield, and with a retail electricity price of USD 0.12, the estimated annual revenue is USD 378.36. The payback period will therefore be 2.8 years compared with purchasing electricity.

7. Conclusions

This work presented a small grid-connected power generation unit for farming systems to support the Bio-Circular-Green Economic (BCG) model in Thailand. The main conclusions are the following:

- A maximum power transmission system of 1.2 kW with a thermal efficiency of 10.7% if the system operates at 1.2 kW.
- Assume that we aim to generate 1.2 kW of electricity for 8 hours each day. Accordingly, this pig farm must have at least 34 pigs.
- The payback period will therefore be 2.8 years.
- The CO emissions of biogas-fed engines decrease with the power output, where CO emissions of less than 1300 ppm at 80% power output are believed to be due to complete combustion. On the other hand, CO emissions with gasohol 95, and LPG are 2000 ppm for all power levels.
- The advantages of the proposed biogas power generation system can be summarized as follows:
 - 1) The system supports a circular economy for agriculture and livestock sector, moving to sustainability.
 - 2) The proposed power generation system is a dispatchable renewable source, which can be used for grid support, and which will be part of the smart grid in the near future.
 - 3) The system is easy to operate, and maintenance of the engines can be done in the community.

8. Acknowledgements

The National Research Council of Thailand supported this work under the Project on Formation of Sustainable Green Communities by Alternative Energy. Panupon Trairat is grateful to the Research and Researchers for Industries (RRI) program and Big Solar Co., Ltd. for sponsoring his doctoral study, grant no. PHD61I0048. Thanks to Ta Manoa Sub District Administration Organization for facilitating the field tests.

9. References

- [1] Palapleevalya P, Poboan C, Mungcharoen T. Development of sustainable consumption and production indicators for industrial sector according to circular economy principles in Thailand. *Interdiscip Res Rev.* 2021;16(6):13-8.
- [2] Edyvean RG, Apiwatanapiwat W, Vaithanomsat P, Boondaeng A, Janchai P, Sophonthammaphat S. The bio-circular green economy model in thailand – a comparative review. *Agr Nat Resour.* 2023;57(1):51-64.
- [3] Energy Policy and Planning office. Thailand power development plan 2018 Rev. 3 [Internet]. 2018 [cited 2019 Nov 15]. Available from: https://www.eppo.go.th/images/Infomation_service/NEWS/2018/PDP_Public_Hearing2018_3.pdf.

- [4] Liu Y, Ma X, Shu L, Hancke GP, Abu-Mahfouz AM. From industry 4.0 to agriculture 4.0: current status, enabling technologies. *IEEE Trans Industr Inform.* 2021;17(6):4322-34.
- [5] Scot MK, Furstenuau LB, Kipper LM, Giraldo FD, López-Robles JR, Cobo MJ, et al. Precision techniques and agriculture 4.0 technologies to promote sustainability in the coffee sector: state of the art, challenges and future trends. *IEEE Access.* 2020;8:149854-67.
- [6] Cheng WM, Liu HJ, Chen R, Chang WC, Yuan JJ, Chen J, et al. A real and novel smart agriculture implementation with IoT technology. The 9th International Conference on Orange Technology (ICOT); 2021 Dec 16-17; Tainan, Taiwan. USA: IEEE; 2021. p. 1-4.
- [7] Aceleanu MI, Șerban AC, Suciu MC, Bițoiu TI. The management of municipal waste through circular economy in the context of smart cities development. *IEEE Access.* 2019;7:133602-14.
- [8] Khotmanee S, Pinsopon U. A study on biogas production potential in Thailand 2019. The 7th International Conference on Engineering–Applied Sciences and Technology (ICEAST); 2021 Apr 1-3; Pattaya, Thailand. USA: IEEE; 2021. p. 269-72.
- [9] Chanathaworn J, Dussadee N. Application of supporting media for improvement of anaerobic digestion performance and biogas production. *Int J Renew Energy.* 2017;12(2):65-74.
- [10] Schlegel M, Kanswohl N, Rossel D, Sakalauskas A. Essential technical parameters for effective biogas production. *Agron Res.* 2008;6(SI):341-8.
- [11] Fathabadi H. Internal combustion engine vehicles: converting the waste heat of the engine into electric energy to be stored in the battery. *IEEE Trans Veh Technol.* 2018;67(10):9241-8.
- [12] Barz M. Biomass technology for electricity generation in community. *Int J Renew Energy.* 2008;3(1):1-10.
- [13] Paenpong C, Pratoomchai N. Performance evaluation of a small spark-ignited engine with an electromagnetic intake valve. *J Res Appl Mech Eng.* 2021;9(1):1-14.
- [14] Rao R, Raju R, Rao M. Experimental investigations on the Mahua fuelled C.I engine with different oxygenates. *Int J Renew Energy.* 2008;3(1):63-70.
- [15] Honda. General purpose engines GX series ed Honda Power Products [Internet]. 2019 [cited 2019 Nov 15]. Available from: <https://engines.honda.com/models/series/gx>.
- [16] Blaabjerg F, Lungeanu F, Skaug K, Tonnes M. Two-phase induction motor drives. *IEEE Ind Appl Mag.* 2004;10(4):24-32.
- [17] Mosaad MI. Optimization of self excited induction generator using constrained particle swarm optimization. *Thammasat Int J Sc Tech.* 2011;16(3):37-45.
- [18] Ojo O, Jimoh AA. Steady-state and dynamic analyses of isolated self-excited induction generators. *Trans South Afr Inst Electr Eng.* 1999;90(1):14-9.
- [19] Hitachi. Hitachi electric motors for industrial application [Internet]. 2010 [cited 2019 Nov 15]. Available from: https://hiem.hitachi.com.my/brochures/pdf/Brochure_ElectricMotor.pdf.
- [20] Somkun S. High performance current control of single-phase grid-connected converter with harmonic mitigation, power extraction and frequency adaptation capabilities. *IET Power Electron.* 2021;14(2):352-72.
- [21] Somkun S, Unbalanced synchronous reference frame control of single-phase stand-alone inverter. *Int J Electr Power Energy Syst.* 2019;107:332-43.
- [22] Somkun S, Chunkag V. Unified unbalanced synchronous reference frame current control for single-phase grid-connected voltage-source converters. *IEEE Trans Ind Electron.* 2016;63(9):5425-36.
- [23] Texas Instruments. TMS320x2806x Microcontrollers Technical Reference Manual [Internet]. 2011 [cited 2019 Nov 15]. Available from: <https://www.ti.com/product>.
- [24] Schneider Electric. EasyLogic PM2200 Series User Manual [Internet]. 2020 [cited 2020 Dec 5]. Available from: <https://www.se.com/th/th/download/document/NHA2778902-01>.
- [25] Späth P. Firebase. In: Späth P, editor. *Pro Android with Kotlin*. Berkeley: Apress; 2022. p. 363-6.
- [26] Mir SB, Lluca GF. Introduction to programming using mobile phones and MIT App inventor. *IEEE Revista Iberoamericana de Tecnologías del Aprendizaje.* 2020;15(3):192-201.
- [27] Mikolajczyk T, Fuwen H, Moldovan L, Bustillo A, Matuszewski M, Nowicki K. Selection of machining parameters with Android application made using MIT App Inventor bookmarks. *Procedia Manuf.* 2018;22:172-9.
- [28] Sutherasak E, Pirompudg W, Sanitjai S. Performance and emissions characteristics of a direct injection diesel engine from compressing producer gas in a dual fuel mode. *Eng Appl Sci Res.* 2018;45(1):47-55.
- [29] Poonnakhun W, Suntivarakorn P, Theragulpisut S, Sookkumnerd C. The effect of biodiesel on diesel engine performance. *KKU Eng J.* 2006;33(3):193-208. (In Thai)
- [30] Kaparaju P, Rintala J. Chap 17 - Generation of heat and power from biogas for stationary applications: boilers, gas engines and turbines, combined heat and power (CHP) plants and fuel cells. In: Wellinger A, Murphy J, Baxter D, editors. *The biogas handbook*. Cambridge: Woodhead Publishing; 2013. p. 404-27.